Developmental Biology 356 (2011) 516–528

Contents lists available at ScienceDirect

Developmental Biology

journal homepage: www.elsevier.com/developmentalbiology

The *tailless* ortholog *nhr-67* functions in the development of the *C. elegans* ventral uterus

Eliana Verghese [a], John Schocken [a], Sandrine Jacob [b], Angela M. Wimer [a], Rebecca Royce [a], Jessica E. Nesmith [a], G. Michael Baer [a], Sheila Clever [a], Elizabeth McCain [a], Bernard Lakowski [b], Bruce Wightman [a,*]

[a] Biology Department, Muhlenberg College, Allentown, PA 18104, USA
[b] Nematode Genetics Laboratory, Department of Neuroscience, Pasteur Institute, 25 rue du Docteur Roux, Paris, 75724, France

ARTICLE INFO

Article history:
Received for publication 10 January 2011
Revised 13 May 2011
Accepted 4 June 2011
Available online 28 June 2011

Keywords:
Notch
Organogenesis
Nuclear receptors

ABSTRACT

The development of the *C. elegans* uterus provides a model for understanding the regulatory pathways that control organogenesis. In *C. elegans*, the ventral uterus develops through coordinated signaling between the uterine anchor cell (AC) and a ventral uterine (VU) cell. The *nhr-67* gene encodes the nematode ortholog of the *tailless* nuclear receptor gene. Fly and vertebrate *tailless* genes function in neuronal and ectodermal developmental pathways. We show that *nhr-67* functions in multiple steps in the development of the *C. elegans* uterus. First, it functions in the differentiation of the AC. Second, it functions in reciprocal signaling between the AC and an equipotent VU cell. Third, it is required for a later signaling event between the AC and VU descendants. *nhr-67* is required for the expression of both the *lag-2/Delta* signal in the AC and the *lin-12/Notch* receptor in all three VU cells and their descendants, suggesting that *nhr-67* may be a key regulator of *Notch*-signaling components. We discuss the implications of these findings for proposed developmental regulatory pathways that include the helix–loop–helix regulator *hlh-2/daughterless* and transcription factor *egl-43/Evi1* in the differentiation of ventral uterine cell types.
© 2011 Elsevier Inc. All rights reserved.

Introduction

The NR2E1/NR2E2 nuclear receptor transcription factors are conserved among animal phyla where they play major roles in regulating development. The *Drosophila* gene *tailless* (*tll*) functions in embryonic body patterning and the development of neurons (Daniel et al., 1999; Jürgens et al., 1984; Pignoni et al., 1990). The vertebrate ortholog of *tailless* (Tlx) functions in the development of limbic and rhinencephalic brain regions in the mouse and is a key regulator of embryonic and adult neural stem cell development (Monaghan et al., 1997; Shi et al., 2004; Yu et al., 1994). The *C. elegans* genome sequencing project identified *nhr-67*, which encodes the nematode ortholog of *tll* (DeMeo et al., 2008; Gissendanner et al., 2004). Like most nuclear receptors, *nhr-67* encodes a protein with a well-conserved DNA-binding domain and a more weakly conserved ligand-binding domain, although ligands have not been identified for any members of the NR2E1/NR2E2 subclass. RNA-mediated interference (RNAi) experiments revealed that *nhr-67*(*RNAi*) animals were slow-growing and displayed cuticle-shedding defects, egg-laying defects (Egl phenotype), and a protruding vulva (Pvl phenotype), suggesting that *nhr-67* plays multiple roles in development (Gissendanner et al., 2004). Fernandes and Sternberg (2007) demonstrated that *nhr-67* plays a role in cell fusion events during vulval morphogenesis, Kato and Sternberg (2009) showed that *nhr-67* functions in the migration of the male linker cell, and Sarin et al. (2009) identified a role for *nhr-67* in neuronal differentiation. In this study, we describe the role of *nhr-67* in regulating development of cells that comprise the ventral *C. elegans* hermaphrodite uterus.

The development of the *C. elegans* uterus has served as a model for understanding the mechanisms of organogenesis. A series of cell–cell signaling events utilize the *Notch* pathway to create the adult hermaphrodite uterus, which consists of sixty cells that contain a lumen and connect to the dorsal side of the vulva (Fig. 1; Newman and Sternberg, 1996; Newman et al., 1996). The anchor cell (AC) of the ventral uterus plays a pivotal role in coordinating the development of the uterus. The AC is generated from one of two equipotent cells in the immature L2 somatic gonad. The cell that does not become the AC becomes a VU (ventral uterine) cell. The selection of which cell executes each fate depends on birth order and reciprocal signaling between a *delta*-like signal, LAG-2, and a *Notch*-like receptor, LIN-12 (Greenwald et al., 1983; Karp and Greenwald, 2003; Kimble and Simpson, 1997). The AC expresses the LAG-2 signal and down-regulates expression of LIN-12 receptor, while the VU cell down-regulates expression of LAG-2. When function of either *lin-12* or *lag-2* is compromised, the VU cell executes an AC fate, resulting in the formation of 2 AC's. Two other somatic gonad cells also serve as VU cells, for a total complement of three VU and one AC in late L2 wild-type animals. While the AC is terminally differentiated in the L2, the three VU

* Corresponding author at: Department of Biology, 2400 Chew St. Allentown, PA 18104, USA. Fax: +1 484 664 3002.
E-mail address: wightman@muhlenberg.edu (B. Wightman).

0012-1606/$ – see front matter © 2011 Elsevier Inc. All rights reserved.
doi:10.1016/j.ydbio.2011.06.007

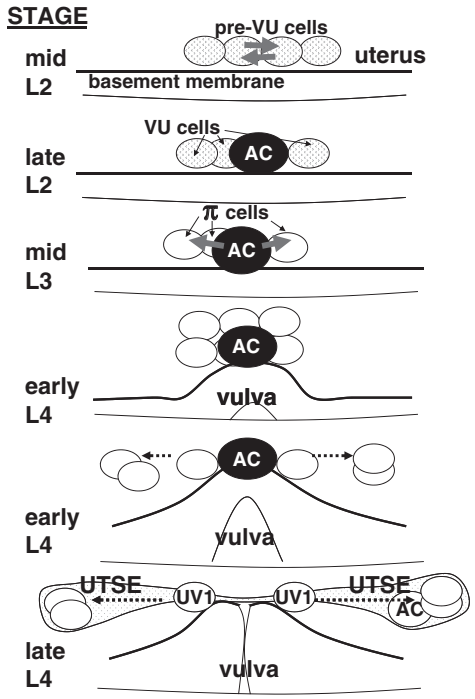

Fig. 1. Summary of ventral uterine development. Larval stages are designated in left column. VU cells are shown as stippled nuclei. The AC is shown in black until it fuses with UTSE. The π cells and their descendants are shown as white nuclei. Cell–cell communication events are designated by solid gray arrows, cellular migrations by broken arrows. The early L3 through late L4 views show the π cells and their descendant cells on one side of the animal only; the total number of π lineage cells is double that shown.

cells divide multiple times during the L3 and L4 stages to produce 36 cells that comprise the ventral uterine tissue and part of the uterine–spermathecal junction (Kimble and Hirsh, 1979).

During the L3 stage, the AC signals using LAG-2 to six adjacent VU descendants via the LIN-12 receptor to execute a single dorsal–ventral division, which is termed the π fate (Fig. 1; Newman et al., 1995, 1996, 2000). The twelve π cell descendants differentiate into four UV1 cells, which will connect directly to the dorsal side of the vulva, and eight cells that fuse to create a large, thin UTSE syncytial cell that forms the ventral surface of the uterus. The six additional VU descendants that do not receive the LAG-2 AC signal execute a default anterior–posterior division and then divide a second time (ρ fate). Following its final role in orchestrating the development of the uterus, the AC "retires" by fusing with the UTSE syncytium during the L4 stage (Newman et al., 1996).

The similarity among the phenotypes caused by *nhr-67* mutations and the phenotypes of mutations in other genes that function in uterine development, combined with a dynamic pattern of *nhr-67* expression in AC and VU cells, suggested that *nhr-67* might function in a *lin-12/Notch* pathway to regulate uterine development. To test this possibility, we identified and studied mutations in the *nhr-67* coding region and promoter, and explored the regulation of *nhr-67* in ventral uterine cells. Our data support a model in which *nhr-67* functions upstream of the *lin-12/Notch* receptor in the VU lineages, upstream of the *lag-2/Delta* signal in the AC, and in a pathway that includes *hlh-2/daughterless* and *egl-43/Evi1* transcription factors to control ventral uterine development at multiple steps.

Materials and methods

Identification and characterization of nhr-67 promoter mutations

During screens for spontaneous mutations with visible phenotypes in a *dog-1*(*gk10*)I background, we isolated a mutation with a partially penetrant Egl and Pvl phenotype superficially similar to the weak *sel-12*(*ar131*) presenilin mutation. Genetic mapping experiments placed *pf2* on LG IV in an interval between SNP_R13[1] and *pkP4085* near *dbP7* (data not shown). *dog-1* encodes a DNA helicase orthologous to the human BACH1/BRIP1/FANCJ gene implicated in Fanconi anemia and certain cancers (Cheung et al., 2002; Youds et al., 2008). Elimination of *dog-1* function leads to a high frequency of deletions starting at long G-rich sequences, especially poly-G stretches, that can form multiple G-quadruplexes when the DNA is single stranded (Cheung et al., 2002; Kruisselbrink et al., 2008; Zhao et al., 2008). We looked for candidate genes in the region that could explain the Egl phenotype and which contained a G-rich sequence in, or near the gene. For each candidate gene we designed primers flanking the G-rich sequences and tested for the presence of deletions in the *pf2* strain (Table S2). No deletions were identified for the Notch ligands *dsl-5* and *dsl-6*, nor for *T01G1.3*, but a small deletion was detected in the promoter region of *nhr-67* by genomic amplification. A stronger Egl mutation with a larger deletion of the *nhr-67* promoter, *pf159*, was recovered in the same screen.

The *pf88* mutation was recovered as a spontaneous mutation arising in the background of a *dog-1*(*gk10*) *I*; *sel-12*(*ty11*) *spr-3*(*pf83*) X strain. The *sel-12*(*ty11*) mutation causes a strong Egl defect and a moderate penetrance Pvl defect (Cinar et al., 2001; Gontijo et al., 2009), similar to a weak *lin-12*(*lf*) allele. The phenotypic effects of *sel-12* mutations are completely suppressed by loss of *spr-3* activity which leads to the de-repression of the transcription of the *hop-1* presenilin gene (Lakowski et al., 2003). The *pf88* mutation causes a nearly 100% penetrant Egl and Pvl phenotype in the *sel-12 spr-3* background, indicating that *pf88* is epistatic to *spr-3* (data not shown). The *pf2*, *pf88* and *pf159* mutations were removed from the presence of all other known mutations in the isolation strains by outcrosses and the presence of the *nhr-67* deletion and absence of *dog-1*(*gk10*) was confirmed by amplification from genomic DNA using specific oligonucleotides (Table S2) before phenotypic characterization. All three deletions start in, or near a C_{18} stretch in the promoter of *nhr-67* which is the presumed site of instability in the *dog-1*(*gk10*) background. The exact breakpoints of each deletion were determined by DNA sequencing (Table S3). The sequences of wild-type *nhr-67* promoter regions (4 kb upstream from start codon) from *C. elegans*, *C. briggsae*, *C. brenneri*, and *C. ramanei* were aligned and compared using the UCSC Multiz Alignment Utility (http://genome.ucsc.edu) and Clustal W (Thompson et al., 1994). Conserved blocks were identified as sequences of at least six nucleotides in length that were perfectly conserved among all four species.

Nematode strains and genetics

C. elegans were cultured and crosses performed as described by Brenner (1974) and Stiernagle (2006). Strains were obtained from the *Caenorhabditis* Genetics Center, the National Bioresource Project of Japan, the *C. elegans* Gene Knockout Consortium, and individual researchers (Table S1). Most strains were constructed using standard Mendelian crosses. An *nhr-67::gfp* extrachromosomal array was obtained from C. Gissendanner (U. La-Monroe) and A Sluder (Scynexis) (Gissendanner et al., 2004). We integrated the array to create transgenes *bwIs5* and *bwIs6* using gamma-irradiation from a Cs source at the University of Pennsylvania Medical School (Mello and Fire, 1995). Strains MU1269 (*nhr-67*(*pf88*)/*nT1qIs51*), MU1270 (*nhr-67*(*pf159*)/*nT1qIs51*), and MU1255 (*nhr-67*(*tm2217*)/*nT1qIs51*), were all created using the same approach. GFP^+ *qIs51nT1* males were mated to homozygous *nhr-67*(*pf88*), homozygous *nhr-67*(*pf159*), and unbalanced heterozygous *tm2217*/+ hermaphrodites (the translocation-linked *qIs51* transgene expresses MYO-2::GFP in the pharynx, but is homozygous lethal; K. Siegfried and J. Kimble, unpublished data). We scored and picked live animals for GFP status using a Nikon SMZ 1500 fluorescent dissecting binocular microscope. Individual GFP^+ F1 hermaphrodites were picked, allowed to reproduce. We tested F1 hermaphrodites individually for the presence of the heterozygous

tm2217 deletion by amplification using the primers that were designed for the original isolation of the deletion (S. Mitani, personal communication; Jansen et al., 1997; Edgley et al., 2002). The heterozygous *pf88* and *pf159* alleles were confirmed by the presence of viable Pvl Egl (protruding-vulva, egg-laying defective) progeny in the F2. Balancing the two strong hypomorphic viable alleles assisted in subsequent strain construction because homozygous mutants mate very poorly as hermaphrodites (due to vulval and uterine defects). The VC419 strain obtained from the *C. elegans* Knockout Consortium had the *ok631* allele balanced *in trans* to *nT1qIs51*. The original strain was back-crossed three times to *nT1qIs51*/+ males to create strain MU1166. We tested complementation of *pf2* and *ok631* as follows: We crossed wild-type males to *ok631*/*nT1qIs51* balanced heterozygotes to generate non-GFP *ok631*/+ males, which were then crossed to *dpy-4* (*e1166*) *nhr-67*(*pf2*) hermaphrodites. We picked non-Dpy hermaphrodites in the F2 and scored them for visible phenotypes. The presence or absence of *pf2* was determined by PCR using primers that flank the deletion. We tested complementation of *pf2* and *mDf7* as follows: *nT1qIs51*/+ males were crossed to *dpy-13*(*e184sd*) *mDf7*/*nT1 let* (*m435*) *IV*;*V* hermaphrodites. F1 progeny that were GFP$^+$ and semi-Dpy were isolated to establish a *dpy-13*(*e184sd*) *mDf7*/*nT1qIs51* balanced strain. Wild-type males were crossed to this strain and non-GFP males picked (*dpy-13*(*e184sd*) *mDf7*/+ males), which were then crossed to *dpy-4*(*e1166*) *nhr-67*(*pf2*) hermaphrodites. From crosses in which the presence of wild-type progeny established successful mating, semi-Dpy hermaphrodites were picked individually and scored for segregation of both the strong Dpy-4 phenotype and the semi-Dpy-13 phenotype at a 1:2 ratio, thus establishing strain MU1271 *dpy-13*(*e184sd*) *mDf7*/*nhr-67*(*pf2*) *dpy-4*(*e1166*) *IV*.

Microscopy

To examine external anatomy by Scanning Electron Microscopy, wild-type and *nhr-67*(*pf88*) animals were fixed in 3% glutaraldehyde (Eisner et al., 1996) and stained in 1% osmium tetroxide following established procedures (Cox et al., 1981; Mackenzie et al., 1978; Morrill, 1986; Peixoto et al., 2000; Shaham, 2006). Samples were viewed with a Topcon ABT-60 Scanning Electron Microscope. In order to evaluate anatomical and cellular characteristics of arrested larvae and the uterus of larvae and adults, we examined wild-type and mutant nematodes using differential interference microscopy (DIC). We employed a Nikon Eclipse TE 2000 U inverted microscope and captured images using a Nikon DMX 1200 camera. To examine and record GFP, YFP and RFP fluorescence patterns we used a Nikon UD Optiphot 2 microscope and captured images using a Nikon DS camera. We cropped images and adjusted for optimum contrast and brightness using Adobe Photoshop software. We evaluated statistical differences in expression of GFP by pairwise comparison using a *t*-test with two-tailed distribution or by chi-square test. We defined "bright" and "weak" expression qualitatively based on our ability to detect expression: "bright" expression was easily observed by direct observation with a 20× objective and could be detected with a 5× objective; "weak" expression could only be observed with a 40× objective and often required the summative effect of digital capture to be clearly resolved.

RNAi

dsRNA-mediated interference (knockdown) was performed by feeding nematodes dsRNA-producing bacteria using standard procedures (Timmons et al., 2001). We obtained plasmids containing *C. elegans* cDNA inserts in vector L4440 flanked by inducible promoters from Open Biosystems (Hunstville, AL) or Geneservice (Nottingham, UK). Experiments were performed either by picking L4 animals or placing synchronized embryos onto RNAi feeding lawns on NGM-IA plates (Ahringer, 2006; Stiernagle, 2006). We performed controls in which each strain was also grown on OP50 bacteria and on HT115 feeding RNAi bacteria on NGM. For all experiments, we confirmed RNAi effectiveness by direct examination of the expected visible phenotypes (e.g. Pvl, Egl, lethal, etc.). Early treatment of nematodes with the *hlh-2*(*RNAi*) feeding strain results in a defect in AC differentiation, however the AC–VU function of *hlh-2* can be assessed by growing animals until the L1–L2 molt on the standard laboratory strain OP50 and then shifting animals to *hlh-2* (*RNAi*) bacteria on NGM-IA plates. To evaluate the effects of L2 *hlh-2* function on *nhr-67::gfp* expression, we performed an OP50-*hlh-2*(*RNAi*) shift experiment (designated *hlh-2*(*RNAi L2*) using a synchronized L1 population of *bwIs6* animals, largely as described by Karp and Greenwald (2003). For experiments that focused on the effects of loss of *nhr-67*, results with *nhr-67*(*RNAi*) were qualitatively and quantitatively similar to the effects caused by the stronger *pf88* and *pf159* mutations (Table 1; data not shown).

Results

Coding region deletions of nhr-67 cause L1 arrest with tail morphology defects

Three mutations that delete a substantial portion of the *nhr-67* coding region have been isolated in systematic gene knockout projects (*ok631*, *tm2172*, and *tm2217*). All three deletions have breakpoints in introns four and six and therefore remove exons five and six completely (Fig. 2). Because exons four and seven would be expected to splice out-of-frame to each other in the absence of exons five and six, the mutant mRNA product should encode a protein that is frame-shifted in the ligand-binding domain. Placing *ok631 in trans* to the viable weak *pf2* allele caused a similar phenotype to placing a large chromosomal deletion *in trans* to the weak *pf2* allele (Table 1). This observation suggests that the *ok631* allele is similar in strength to a complete deletion of the entire *nhr-67* gene, consistent with it being a null allele, at least as regards function in the egg-laying system.

In order to investigate the function of *nhr-67*, we examined homozygous *ok631* and *tm2217* animals produced from balanced strains. Homozygous mutants usually arrested development as embryos or L1 larvae, as is the case for *tll* mutants in *Drosophila*. Less than 10% of *tm2217* homozygous animals developed to adulthood. All *tm2217* homozygous escaper adults had protruding vulva (Pvl) and egg-laying defective (Egl) phenotypes, and produced a small number (1–5) of progeny that invariably arrested at or before the L1 stage. In contrast to *tm2217*, we were unable to recover homozygous *ok631* adult escapers. This may reflect the fact that the *ok631* deletion, but not the *tm2217* deletion, removes a portion of a predicted non-coding RNA, C08F8.10, which is located in intron four, or a difference in strain background between *ok631* and *tm2217*. The observation that all escaper homozygous *tm2217* animals display Egl and Pvl phenotypes confirms the phenotypes obtained by RNAi-based studies of *nhr-67* function (Fernandes and Sternberg, 2007; Gissendanner et al., 2004).

We examined arrested homozygous *nhr-67* (*ok631*) and *nhr-67* (*tm2217*) L1 larvae by light microscopy to determine if loss of *nhr-67* results in major effects on anatomy (Fig. 3). Arrested L1 larvae had grossly normal pharynxes, intestine, and cuticular alae. They were

Table 1
Phenotypes of *nhr-67* mutants and RNAi knockdown.

Genotype	% Adult phenotype				N
	WT	Pvl	Egl	Pvl Egl	
Wild-type	100	0	0	0	47
nhr-67(*RNAi*)	11	8	18	62	70
nhr-67(*pf159*)	9	7	18	64	55
nhr-67(*pf88*)	0	1	23	76	66
nhr-67(*pf2*)	29	3	24	42	66
nhr-67(*pf2*)/*nhr-67*(*ok631*)	24	0	33	44	55
nhr-67(*pf2*)/*mDf7*	21	2	42	35	146

Percentages do not necessarily sum to 100% due to rounding.

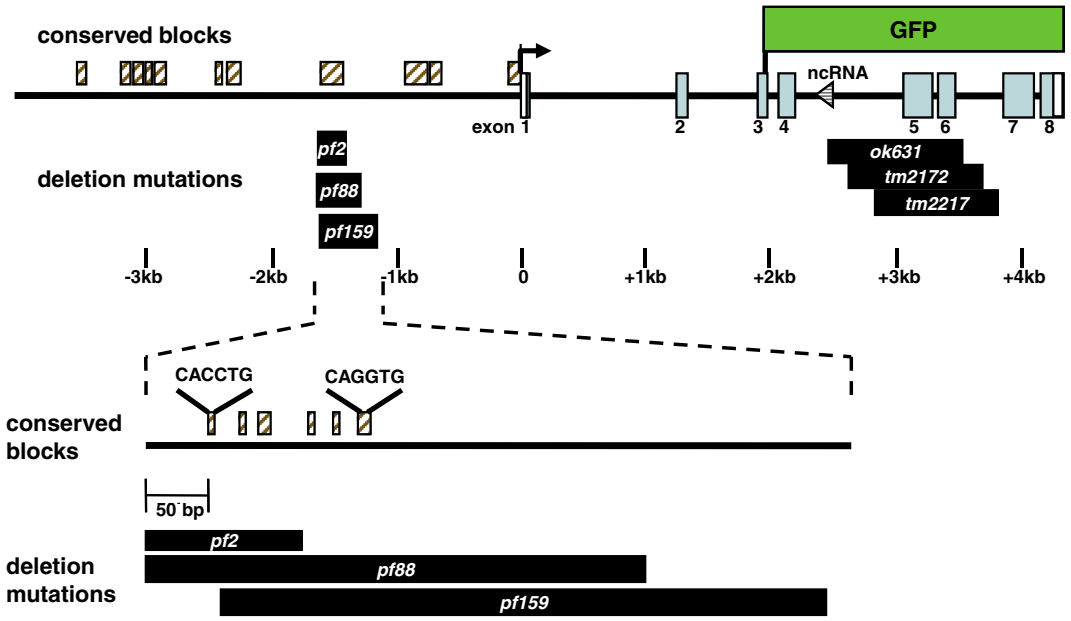

Fig. 2. Genomic organization of the *nhr-67* gene. Schematic of the *nhr-67* gene. The first nucleotide of the ORF start codon is designated as the 0 position, with positions in kb below the line. Boxes on the line designate exons, numbered 1–8, with the coding region shaded. A line-filled arrow within intron 4 designates the position of the predicted ncRNA, C08F8.10. Shaded boxes above the line indicate regions that consist of multiple blocks of sequences that are each at least six bp long and perfectly identical among *C. elegans*, *C. briggsae*, *C. brenneri*, and *C. ramanei*. The locations of two perfectly conserved CAGGTG HLH-2 binding sites are shown above the line. Black boxes below the line indicate the extent of deleted DNA in *nhr-67* mutants. The location of the translation fusion to GFP in the *nhr-67::gfp* reporter used in this study (Gissendanner et al., 2004) is shown above the line.

able to move, but appeared slightly uncoordinated in comparison to heterozygous sisters. Over 90% of arrested larvae did not have any bacteria in their gut, suggesting that most *nhr-67* homozygous mutants are unable to eat. Both *nhr-67* (*ok631*) and *nhr-67* (*tm2217*) arrested L1 larvae displayed variable defects in tail morphology, including kinks, bulges, and forks (Fig. 3B). Tail morphology defects were not observed in later stage escapers, suggesting that either the defect is confined to an event in late embryogenesis that can be resolved at the L1/L2 molt or that escapers emerge from a small population of mutants that escape all cuticular defects at all stages.

Deletions in the nhr-67 promoter cause defects in the development of the vulva and ectoderm

We identified three viable mutations that mapped to the *nhr-67* promoter region. The *pf2*, *pf88* and *pf159* alleles delete 127, 398, and 494 bp, respectively, of overlapping portions of the *nhr-67* promoter in a region that lies between 1200 bp and 1700 bp upstream of the predicted *nhr-67* start codon (Fig. 2; Table S3). This region includes six blocks of sequences that are conserved among four nematode species, suggesting that multiple promoter cis-regulatory elements are missing from each deletion. The *pf2* deletion removes three conserved blocks, the *pf159* deletion five conserved blocks, and the *pf88* deletion all six conserved blocks.

Animals that are homozygous for any of these three recessive hypomorphic mutations are viable and display Egl and Pvl phenotypes (Table 1; Figs. 3D, E). Both phenotypes reflect a defect in the development of the vulva and/or uterus. The larger *pf88* and *pf159* deletions cause considerably stronger phenotypes than the smaller *pf2* deletion, suggesting that loss of the three proximal conserved blocks has a significant effect on transcription of the *nhr-67* gene. The *pf2* mutation fails to complement *in trans* the *ok631* deletion of the *nhr-67* ORF (Table 1), demonstrating that the Egl and Pvl phenotypes are a consequence of the effect of the promoter deletion on *nhr-67* rather than a neighboring gene. The larger promoter deletions, *pf88* and *pf159,* cause a low-penetrance (2–5%) sterility, indicating that *nhr-67* may also be required for normal germ-line development, and a low-penetrance (about 5%) cuticular morphology defect in younger larva, presenting as variably positioned bulges and lumps (Fig. 3C). Taken together, these observations suggest that *nhr-67* functions in critical developmental processes in multiple tissues.

nhr-67 functions in ventral uterine development

Because the Pvl and Egl phenotype suggested that *nhr-67* might function in uterine development, we examined *nhr-67* mutants for defects in uterine cell types. In mid-L4 wild-type hermaphrodites, the UTSE syncytium is normally visible as a very thin cell layer atop the separated dorsal-most VulF vulval cells (Fig. 3F). In contrast, *nhr-67* mutants have a thick cell layer atop the mid-L4 vulva and the VulF cells do not separate (Figs. 3G, H), indicating that *nhr-67* is required for normal UTSE morphogenesis. We also found that the AC fails to fuse with UTSE (Figs. 3G, H), a phenotype that is often observed in other mutants when UTSE development is defective (Hanna-Rose and Han, 1999). In order to examine the differentiation of the 4 UV1 cells, we examined strains that carried an *ida-1::gfp* transgene that is expressed in the UV1 cells (Fig. 3I; Zahn et al., 2001). *nhr-67* mutants have dramatically reduced numbers of UV1 cells expressing *ida-1::gfp* (Fig. 3J). When UV1 cells were observed, they were often abnormal in terms of position and morphology (data not shown). Therefore, both mature uterine cell types derived from the π lineage are defective in *nhr-67* mutants.

nhr-67 is expressed dynamically in the developing uterus

The defects in the development of the ventral uterus could be accounted for by *nhr-67* function in the AC, the π cells, and/or the VU cells, which give rise to the π cells. In order to identify potential sites of *nhr-67* function, we examined transgenic nematodes carrying an *nhr-67::gfp* translational fusion that includes 6 kb of upstream promoter sequence and the first three exons (Fig. 2; Gissendanner et al., 2004). The translational fusion does not include the entire *nhr-67* DNA-binding domain and did not rescue *nhr-67* Pvl, Egl, or cellular phenotypes (data not shown). *nhr-67::gfp* was expressed at all postembryonic stages in neurons of the head; the details of the neuronal expression have been reported by Sarin et al. (2009). We did

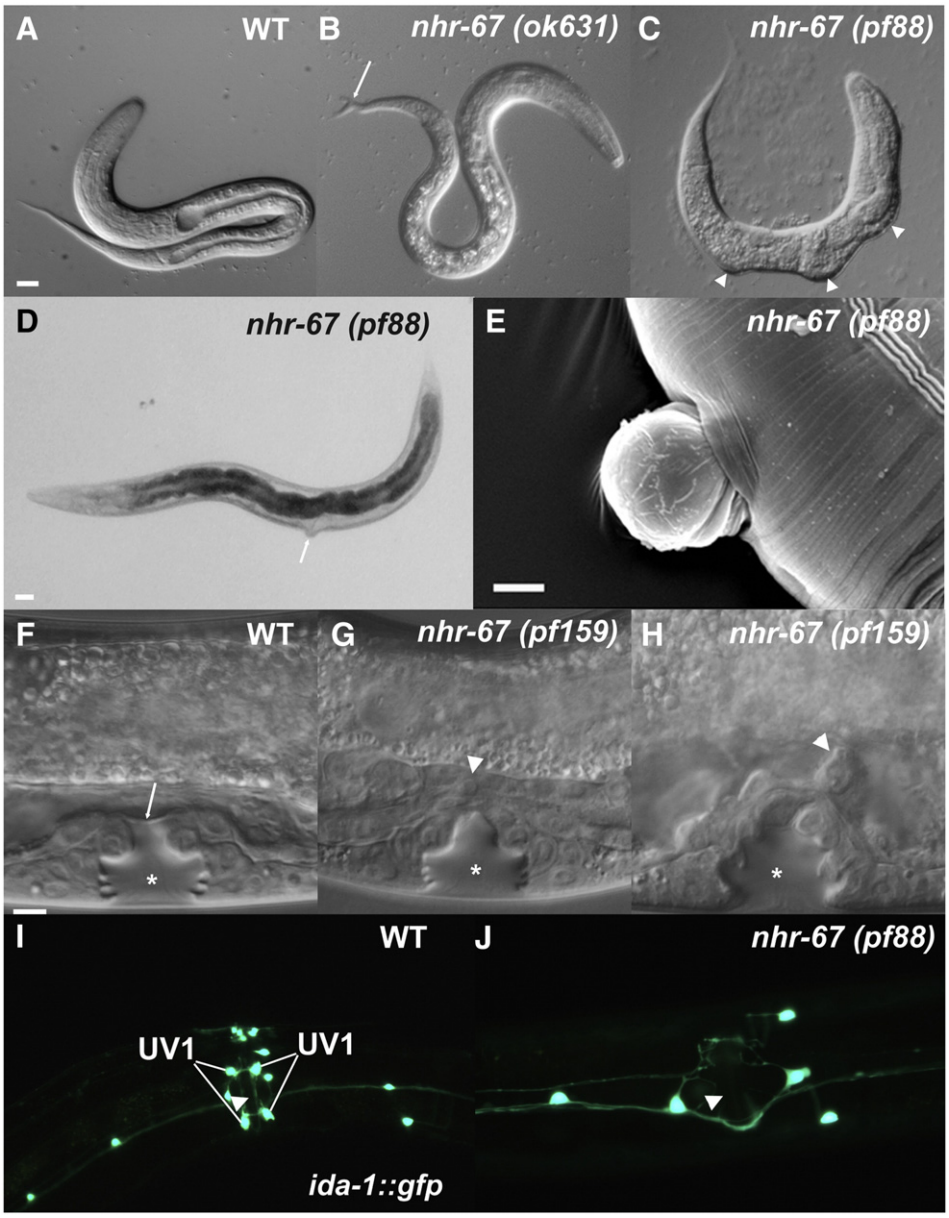

Fig. 3. Morphology and uterine defects of *nhr-67* mutations. DIC Nomarski images (A–C, F–H), bright field image (D), scanning electron micrograph (E) and fluorescence microscopy images (I, J) of wild-type (A, F, I) and *nhr-67* mutants (B–E, G–H, J). L1 arrest tail defect (B) is identified by arrow. Cuticule morphology bulges (C) are identified by arrowheads. A sterile Pvl animal is shown in (D), with a vulval protrusion indicated by the arrow. Note the absence of gonadal arms. Close-up of a Pvl protrusion (E). In (F–H), arrow indicates the thinned UTSE tissue that separates the vulval lumen (asterisk) from uterine lumen, and arrowheads identify the unfused AC. Expression of *ida-1::gfp* in the UV1 cells (labeled) of the ventral uterus (I, J). In addition to the four UV1 cells, the *ida-1::gfp* transgene is also expressed in several neurons. A, B, C, scale bar = 10 μm. D, scale bar = 30 μm. E, scale bar = 5.3 μm.

not observe any *nhr-67::gfp* expression in uterine or vulval precursors in embryos or L1 larvae. In the L2 stage, we observed *nhr-67::gfp* expression in the 4 pre-VU precursor cells (Z1.ppa, Z1.ppp, Z4.aaa, Z4.aap) that become the AC and the three VU cells that give rise to the ventral uterus (Fig. 4A). Expression of *nhr-67::gfp* in the 4 pre-VU precursor cells appeared at or shortly after their birth. In the mid- to late-L2 stage, expression of *nhr-67::gfp* in the three VU cells decreased, while remaining at high levels (or possibly increasing) in the AC (Fig. 4B). This change in *nhr-67* regulation was roughly coincident with the AC–VU *lin-12/Notch*-based signaling event that specifies AC identity. During the L3 and early L4 stages, we observed consistent and continual bright *nhr-67::gfp* expression in the AC and more variable weak levels of expression in the six adjacent π cells (Fig. 4C). We very rarely detected *nhr-67::gfp* expression in all 12 π cells after their dorsal–ventral division. From early L4 through adulthood, we observed weak expression of *nhr-67::gfp* in all 8 UTSE cells or syncytium (Fig. 4D), suggesting that expression is turned off in all π cells after their division and then re-expressed later in UTSE. Expression of *nhr-67::gfp* was observed in the UTSE before AC fusion, indicating that it does not reflect GFP introduced into UTSE by fusion of the AC to UTSE. Bright expression of *nhr-67::gfp* in the AC nucleus was not observed after mid-L4, indicating that it is reduced after fusion of the AC with the UTSE syncytium. We did not observe expression of *nhr-67::gfp* in vulval cells at any stage using our transgenic reporter, although Fernandes and Sternberg (2007) have demonstrated expression of *nhr*-67 in a subset of vulval cells during morphogenesis in the L4 stage using a transgenic reporter that includes intron 4. An *nhr-67::mCherry* reporter (Sarin et al., 2009) that rescues *nhr-67*(*ok631*) mutants for viability, Egl and Pvl defects shows the same uterine pattern that we report here, except for the late L4 and adult UTSE expression (data not shown). Therefore, the expression pattern we have described should include expression of

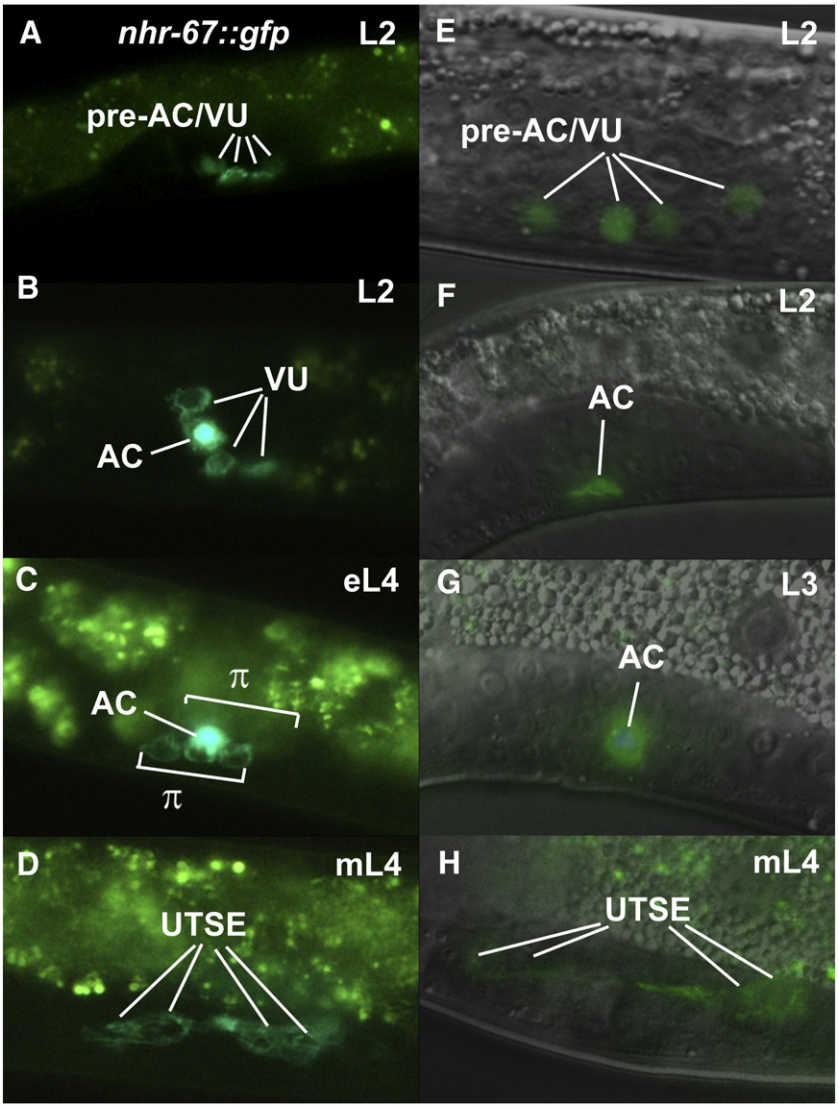

Fig. 4. Expression of *nhr-67* in the developing ventral uterus. Expression of *nhr-67::gfp* in wild-type animals during L2, L3, and L4 stages. (A–D) GFP fluorescence microscopy. (E–H) GFP fluorescence overlays on DIC images. A–D and E–H are not matched images of the same animals. (A, E) Mid L2 larva showing GFP fluorescence in the four pre-AC/VU precursor cells. (B, F) Late L2 larva showing GFP fluorescence in the AC and three VU cells (not visible in DIC overlay), after AC–VU signaling. Early L3 larva are similar. (C) Early L4 and (G) Late L3 larva showing fluorescence in the AC and six adjacent π cells (not visible in DIC overlay). (D, H) Mid-L4 larva showing fluorescence in the UTSE cells. The AC has either fused with UTSE or is no longer expressing *nhr-67::gfp*. The positions of cells are altered from wild-type positions due to the presence of the co-transforming marker *rol-6*, which causes the body to corkscrew around the long axis. Low-level expression of NHR-67::GFP protein in the UTSE and π cells was typically cytoplasmic, but this is probably an artifact of the preferential localization of the GFP fusion protein rather than an indication of different subcellular localization of the endogenous NHR-67 protein. The *nhr-67::gfp* fusion used for this study does not include the entire DNA-binding domain (Fig. 2; Gissendanner et al., 2004), and a full-length *nhr-67::mCherry* transgene displays the expected nuclear localization (Sarin et al., 2009). Anterior is to the left. All images are side views with ventral at bottom, except panel B, which is a ventral view, and panel C, which is an oblique ventral view.

nhr-67 that is relevant to understanding function in uterine development. These data demonstrate that *nhr-67* is dynamically expressed in the developing uterus, and suggests that *nhr-67* function in the AC, VU, and/or π cells may contribute to the defect in uterine development in *nhr-67* mutants.

nhr-67 functions in the AC–VU decision

The early differential expression of *nhr-67::gfp* in the AC and VU cells in late L2 suggested the possibility that *nhr-67* might function in the AC–VU decision. We examined whether *nhr-67* functioned in the development of the AC and/or the AC–VU decision by testing the effect of *nhr-67* mutations or RNAi knockdown on markers of AC identity. The *lin-3* gene encodes an EGF-like signaling molecule that is expressed in the AC and in the three L2 VU cells (Hwang and Sternberg, 2004), following a pattern that is very similar to that of *nhr-67*. Later stage expression of *lin-3* in VU descendants was weak and variable, but expression in the AC remains high (Fig. 5A). Animals subjected to *nhr-67* (*RNAi*) knockdown and *nhr-67* hypomorphic mutants displayed robust expression of *lin-3::gfp* in AC's at stages L2–L4 (Figs. 5A, B; Table 2). In addition, the morphology of the AC during the L3 stage was superficially normal. The presumptive VU cell of L2 and L3 *nhr-67*(*RNAi*) animals and *nhr-67* mutants often displayed a high level of *lin-3::gfp* expression, consistent with upregulation of *lin-3* in the VU cells when *nhr-67* is compromised (Fig. 5B; Table 2). Instead of the single brightly fluorescing AC observed in wild-type animals, 33% of *nhr-67* (*RNAi*) animals displayed two bright cells, often closely adjacent to each other, which both displayed AC-like morphology. In some cases, two adjacent AC-like cells could be seen invading into the underlying ectodermal vulval precursor tissue (data not shown), indicating that both cells were behaving as bonafide AC's. During the late L4 stage, the *lin-3::gfp*-expressing AC of *nhr-67*(*RNAi*) and mutant animals persisted, apparently unable to fuse with the defective UTSE (Table 2). We obtained similar results when we examined the expression of *cdh-3* (Figs. 5C, D; Table 2), which encodes a cadherin that is expressed in the AC beginning

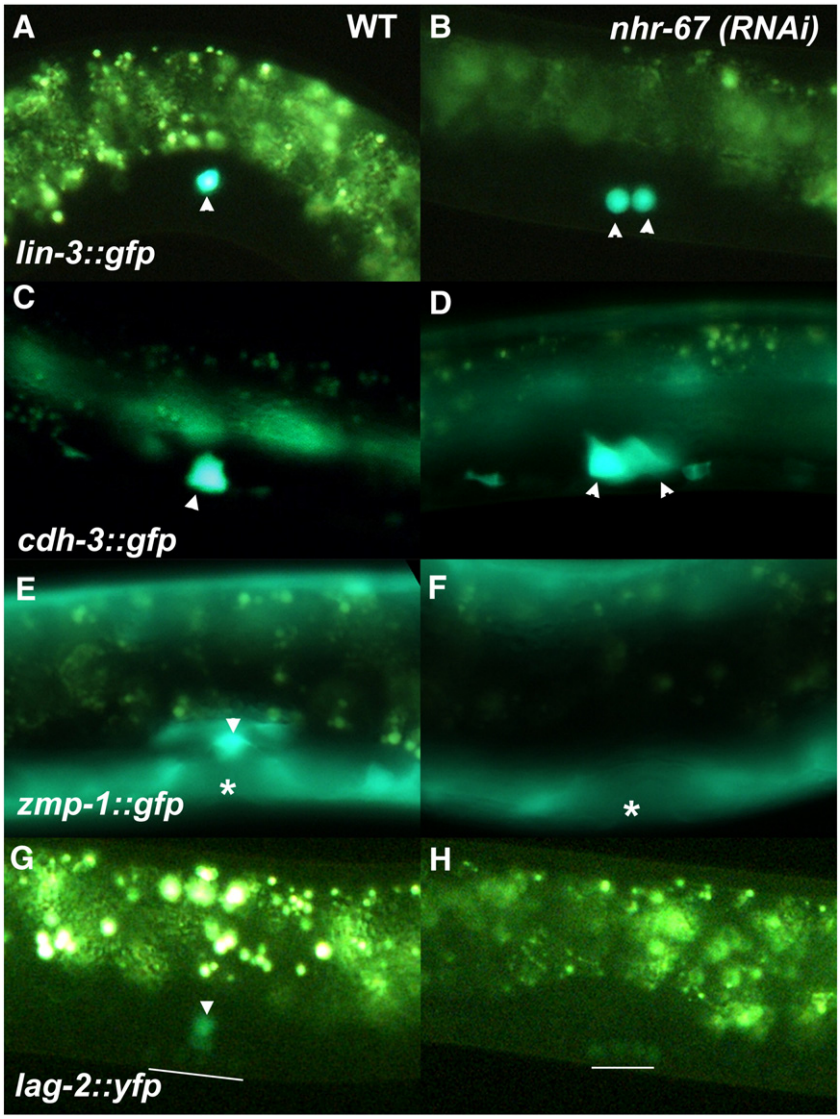

Fig. 5. *nhr-67* functions in the AC–VU decision and AC differentiation. *lin-3::gfp* (A, B), *cdh-3::gfp*(C, D), *zmp-1::gfp* (E, F),and *lag-2::yfp* (G, H) fluorescence in wild-type (A, C, E, G) and *nhr-67*(*RNAi*) knockdown (B, D, F, H) animals. Panels A–D and G–H show L3 animals. Panels E and F show early L4 animals. Arrowheads identify AC's. Asterisks identify the lumen of the developing vulva. Solid line in panels G and H identifies four vulval precursor cells, which also express the *lag-2::yfp* transgene.

in the L3 stage (Inoue et al., 2002; Pettitt et al., 1996). These data demonstrate that multiple markers of AC identity are expressed in the presumptive VU cell. Therefore, when *nhr-67* function is compromised, the presumptive VU cell is unable to respond to, or does not receive, the LAG-2 signal from the AC and adopts an AC identity.

Table 2
Expression of genes in the AC in *nhr-67* mutants and RNAi knockdown.

Larval stage	L3			Mid L4	N
Expression pattern genotype	% 1 AC	% 2 AC	% 0 AC	% retained AC	
lin-3::gfp	100	0	0	7	149
lin-3::gfp; nhr-67(pf88)	58	38	4	23	113
cdh-3::gfp	100	0	0	2	89
cdh-3::gfp; nhr-67(RNAi)	34	65	0	67	41
zmp-1::gfp	87	0	13	0	51
zmp-1::gfp; nhr-67(RNAi)	48	12	41	23	95
lag-2::yfp	95	0	5	0	62
lag-2::yfp; nhr-67(RNAi)	56	7	38	0	108
egl-43::gfp	97	0	3	5	76
egl-43::gfp; nhr-67(RNAi)	70	15	15	38	64

Percentages do not necessarily sum to 100% due to rounding.

nhr-67 functions in AC differentiation

In contrast to *lin-3* and *cdh-3*, other markers of AC identity showed a loss of expression when *nhr-67* was compromised. *zmp-1* encodes a zinc metalloprotease, which is expressed in the AC beginning in the L3 stage, at about the same time as *cdh-3* (Inoue et al., 2002; Pettitt et al., 1996; Sherwood et al., 2005; Sherwood and Sternberg, 2003). With a *zmp-1::gfp* reporter, fluorescence in a second AC was present in some L3 *nhr-67* (*RNAi*) animals, but at a lower penetrance than observed for *lin-3::gfp* and *cdh-3::gfp* (Figs. 5E, F; Table 2). Expression of *zmp-1::gfp* in the AC was weaker and sometimes entirely absent in *nhr-67*(*RNAi*) treated animals (Figs. 5E, F; Table 2). Thus a general loss of *zmp-1* expression in *nhr-67*(*RNAi*) animals may account for the lower penetrance of the apparent two AC phenotype when *zmp-1::gfp* was used as a marker of AC identity. We also observed a modest loss of AC expression coupled with a two AC phenotype when we examined expression of the transcription factor *egl-43* (Table 2). In addition, the AC's of *nhr-67* (*RNAi*) larvae display a defect in invasion of the basement membrane that separates the AC from the vulval tissue below it (Sherwood and Sternberg, 2003; D. Matus and D. Sherwood, personal communication). These results indicate that *nhr-67* is required for normal levels of *zmp-1* expression and some cellular properties of the AC, indicating that *nhr-67*

Table 3
Expression of *nhr-67::gfp* in the AC, VU cells, and π cells.

Stage	Late L2		L3				N
Expression pattern	% 2 bright cells	Avg (±SD) number AC/VU cells	% 1 AC	% 2 AC	% 0 AC	Avg (±SD) number π cells	
Wild-type	6	3.5 (±0.9)	91	0	8	2.5 (±2.5)	133
hlh-2(RNAi)	*18	3.4 (±1.0)	*12	*2	*86	1.6 (±2.4)	134
hlh-2(RNAi L2)	nd[a]	nd[a]	*49	*24	*28	nd[a]	80
egl-43(RNAi)	*18	3.2 (±1.1)	*43	*22	*35	*1.3 (±1.3)	129
lin-12(RNAi)	*28	3.1 (±1.2)	*49	*41	8	2.1 (±1.1)	101
lag-1(RNAi)	*11	3.3 (±1.0)	85	*12	4	1.7 (±2.4)	105
sel-12(ar131)	7	3.8 (±0.7)	92	0	8	2.5 (±2.1)	47

Percentages do not necessarily sum to 100% due to rounding.
* Significantly different from *wild-type* transgene background at $p<0.05$.
[a] Not determined. We did not score AC or π cell phenotypes for *hlh-2(RNAi L2)* animals.

functions in the differentiation of the AC as well as being required for the VU fate during the AC–VU decision.

The observation that *nhr-67* functions in some aspects of AC development raises the possibility that its function in the AC–VU decision may depend on *nhr-67* regulating the expression of the *lag-2* ligand in the AC. To test this possibility, we examined the expression of a *lag-2::yfp* reporter construct (I. Greenwald, personal communication; Wilkinson et al., 1994) when *nhr-67* function is compromised. The expression of *lag-2::yfp* was absent from the AC of 38% of *nhr-67 (RNAi)* L3 animals (Figs. 5G, H; Table 2), and the intensity of *lag-2::yfp* fluorescence was reduced in many *nhr-67(RNAi)* larvae that did show detectable expression. As with *zmp-1*, a low penetrance two AC phenotype was still apparent when *lag-2::yfp* was used as a marker of AC identity. Taken together these results support the conclusion that loss of *nhr-67* results in both a defect in AC–VU signaling and a defect in AC differentiation. Furthermore, the loss of *lag-2* expression could contribute to the defect in AC–VU signaling, since *lag-2* encodes the signal.

Relationship between nhr-67 and the AC development transcription factors hlh-2/daughterless and egl-43/Evi1

The observations that *nhr-67* is expressed relatively early in all four pre-VU cells of the L2 and functions in both AC differentiation and the AC–VU decision suggested that it might depend on transcription factors known to function in the earlier steps in AC development. To address this question, we examined the dependence of *nhr-67::gfp* on the transcription factors *hlh-2* and *egl-43*, both of which have been shown to play a role in early AC development. The *hlh-2* gene encodes a *C. elegans* helix–loop–helix transcription factor that is the ortholog of the *daughterless* gene of *Drosophila melanogaster* (Krause et al., 1997). It functions in multiple steps in ventral uterine development. First, during the L1 stage, *hlh-2* functions in the pre-VU cells to regulate competency to develop into an AC (Karp and Greenwald, 2004). In the absence of *hlh-2* function, the AC is unable to differentiate and becomes a VU-like cell. Second, during the L2 stage, *hlh-2* functions in the AC–VU decision to regulate VU development, in part by positively regulating the expression of the *lag-2* ligand in the AC (Karp and Greenwald, 2003). Therefore, when *hlh-2* function is reduced by RNAi during L2, a two AC phenotype results due to the loss of *lag-2* signal to the VU. When we reduced *hlh-2* function during L1 by RNAi, we observed no significant effect on the number of pre-VU cells that expressed *nhr-67::gfp* in the L2 (Table 3). We also observed a low penetrance two bright AC phenotype, which may reflect rare animals that escaped the early *hlh-2* RNAi effect on AC differentiation, but suffered from L2 RNAi effects on the AC–VU decision. During L3, we observed a significant loss of bright AC-like *nhr-67::gfp* expression (Figs. 6A, B; Table 3), consistent with the expectation that the AC has been converted into a VU-like cell. When we grew animals on non-RNAi bacteria until the L1 molt and then shifted them to *hlh-2* RNAi bacteria (designated *hlh-2(RNAi L2)*), we observed animals with two bright *nhr-67::gfp* expressing AC's, as we would expect due to the L2 AC–VU defect (Fig. 6C; Table 3). Therefore, loss of *hlh-2* at the L2 molt results in conversion of the VU cell into an AC, with concomitant increase in expression of *nhr-67*. We also observed a significant proportion of *hlh-2(RNAi L2)* animals that had no *nhr-67::gfp* expression in the gonad, however these animals also did not have clearly differentiated AC's on the basis of DIC morphology (data not shown), indicating that reduction of *hlh-2* in these animals compromised the earlier *hlh-2* function in pre-AC competency (Karp

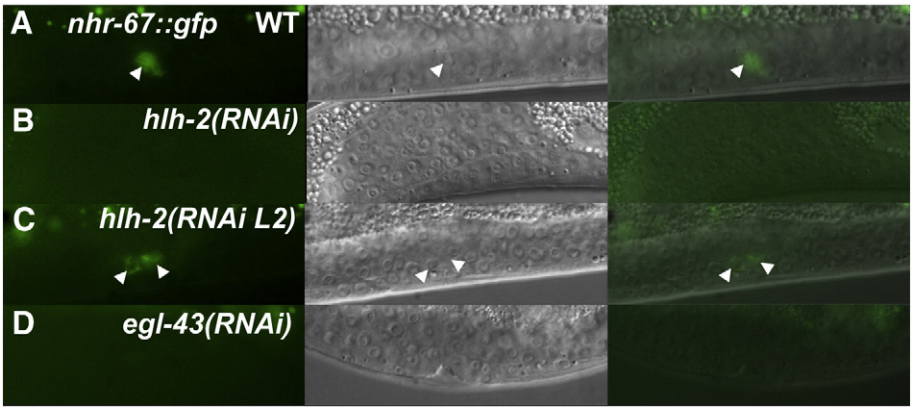

Fig. 6. Expression of *nhr-67* depends on *egl-43* and *hlh-2*. *nhr-67::gfp* fluorescence in (A) wild-type, (B) *hlh-2(RNAi)*, (C) *hlh-2(RNAi L2)*, and (D) *egl-43 (RNAi)* larvae. The left column shows GFP fluorescence, the middle column matched DIC micrographs, and the right column matched DIC micrographs with GFP fluorescence overlays. Arrowheads identify the positions of AC's. Panels A–C show L3 animals. Panel D show an early L4 animal. The gonad of *hlh-2(RNAi)* animals displays a highly abnormal morphology due to pleiotropic requirements for *hlh-2* in gonadogenesis (Karp and Greenwald, 2004). Brightness of panels B and D was intentionally increased to emphasize the lack of GFP fluorescence. Panels B shows a modest twisting of the body due to the presence of the *rol-6* cotransforming marker. Ventral is at the bottom and anterior to the left for all images.

and Greenwald, 2004). Thus we were not able to "decouple" *hlh-2* function in regulating *nhr-67::gfp* expression and *hlh-2* function in AC differentiation. This observation suggests that the loss of *nhr-67::gfp* expression in *hlh-2*(*RNAi*) animals is intimately associated with *hlh-2* function in establishing AC competency rather than reflecting *hlh-2* function in positively regulating *nhr-67* expression in an otherwise normal AC.

The *egl-43* gene encodes a *C. elegans* homolog of the EVI1 proto-oncogene transcription factor (Garriga et al., 1993). The vertebrate EVI1 zinc-finger transcription factor functions in regulating development in multiple tissues, including the peripheral nervous system (Hoyt et al., 1997; Lopingco and Perkins, 1996). Like *hlh-2* and *nhr-67*, *egl-43* plays multiple roles in development, including regulating the AC–VU decision, expression of *zmp-1* in the AC, and invasive behavior of the AC (Hwang et al., 2007; Rimann and Hajnal, 2007). The specific array of AC phenotypes caused by loss of *egl-43* are strikingly similar to those we describe for *nhr-67*: loss of *zmp-1* expression, but not *cdh-3* expression, and a failure to invade vulval tissue and fuse with UTSE. HLH-2 appears to be a direct transcriptional regulator of *egl-43* transcription, binding to a CACCTG "E-box" located in an *egl-43* enhancer that directs expression of *egl-43* in the AC (Hwang et al., 2007). While AC differentiation by several criteria is clearly defective when *egl-43* function is compromised, it is not known whether the presumptive AC is converted into a bona fide VU cell. To examine the consequences of loss of *egl-43* for *nhr-67* expression, we examined *nhr-67::gfp* animals that were subjected to *egl-43*(*RNAi*). Reducing *egl-43* function resulted in an increase in the two bright AC *nhr-67::gfp* phenotype in L2, but no change in the overall number of pre-VU cells, indicating that *egl-43* is not required for early *nhr-67* expression (Table 3). However, during the L3 we observed a two bright AC *nhr-67::gfp* expression phenotype in some animals coupled with a loss of *nhr-67::gfp* expression in both the presumptive AC and VU descendants (Fig. 6E; Table 3). We interpret this to mean that in some *egl-43*(*RNAi*) animals the AC–VU decision fails, resulting in two bright *nhr-67::gfp*-expressing AC's, while in other animals AC differentiation itself is compromised and bright *nhr-67::gfp* expression is not observed. The latter result is very similar to what is observed with *zmp-1* expression in *egl-43*(*RNAi*)-treated animals (Hwang et al., 2007). These data suggest that maintenance of *nhr-67* expression in the AC and VU descendants may depend on *egl-43*. The *hlh-2* and *egl-43* effects on *nhr-67* expression coupled with the similarity in defects in AC differentiation among *hlh-2, egl-43* and *nhr-67*, raises the possibility that *nhr-67* functions in a pathway with both transcriptional regulators in regulating AC differentiation.

The *lin-29* transcription factor functions in maintaining *lag-2* expression in the AC (Newman et al., 2000). Given that *nhr-67* is also required for *lag-2* expression in the AC, we examined the possibility that *nhr-67* expression in the AC might depend on *lin-29* in addition to *hlh-2* and *egl-43*. In contrast to the results we obtained with both *hlh-2* and *egl-43*, we observed no loss of *nhr-67::gfp* expression in the AC of *lin-29* (*RNAi*) animals (data not shown). Therefore, regulation of *nhr-67* does not appear to depend on *lin-29*, which is consistent with an earlier role for *nhr-67* in AC development.

The ventral uterine cells of the π lineage require nhr-67

Because the AC also signals to the adjacent VU descendants during the L3 to induce the π lineage, we hypothesized that the π cells would also be defective when *nhr-67* is compromised. Like the AC–VU signaling event during L2, the AC-π signaling event during L3 depends upon a LAG-2 signal from the AC and a LIN-12-mediated response in the responding cells (Newman et al., 1995). Two transcription factors have been shown to play important roles in the execution of uterine π cell fates and serve as early markers of π lineage induction. The Sox domain transcriptional factor gene *egl-13* functions in the execution of π cell fates (Cinar et al., 2001; Hanna-Rose and Han, 1999), and the LIM homeobox gene *lin-11* is required for the normal differentiation of the UTSE cells (Newman et al., 1999). Genetic studies have demonstrated that *egl-13* and *lin-11* are both downstream of *lin-12*. Expression of both *egl-13::gfp* and *lin-11::gfp* transgenes in the π lineages of *nhr-67* mutants was markedly reduced, both in the number of cells observed and in the brightness of fluorescence (Fig. 7; Table 4). The loss of *egl-13::gfp* and *lin-11::gfp*-expressing cells was observed at both late L3, when the π cells receive the LAG-2 signal and in early L4 after they have executed their characteristic division (Table 4). When *egl-13::gfp*-expressing cells were observed in later L4

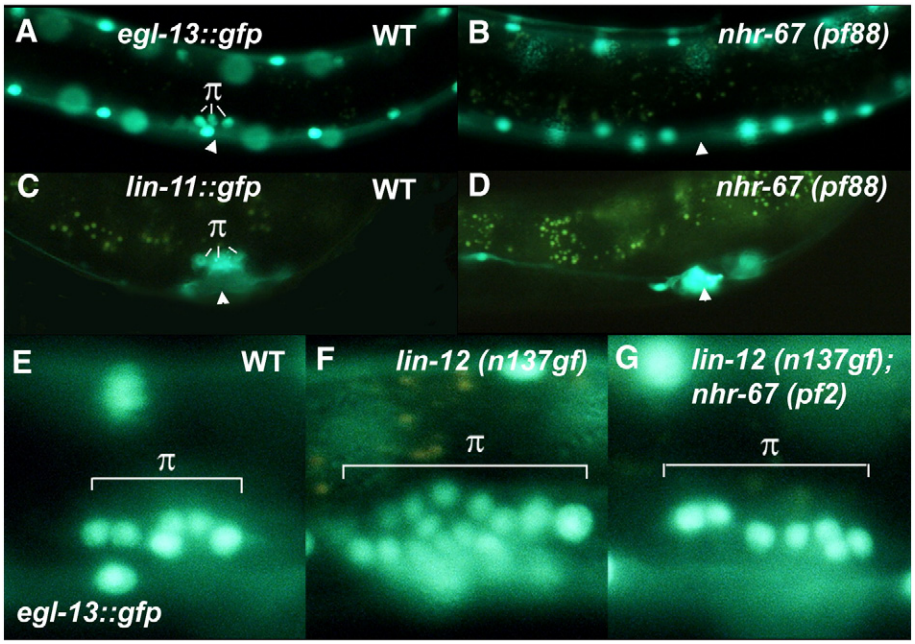

Fig. 7. Defects in expression of genes in the π lineages of *nhr-67* mutants. Fluorescence microscopy showing expression of *egl-13::gfp* (A, B, E–G), and *lin-11::gfp* (C, D) in wild-type (A, C, E), *nhr-67* (*pf88*) (B, D), *lin-12*(*n137gf*) (F), and *lin-12*(*n137gf*); *nhr-67*(*pf2*) (G) backgrounds. (A, B) Side view of L3 animals. (C–G) Side view of early L4 animals. The location of the developing vulva is indicated in each figure with an arrowhead, and π lineage cells are labeled. Anterior is to the left.

Table 4
Expression of genes in the π lineage.

Genotype	Late L3 (6π)			Early L4 (12π)				N
	% WT (5–8π)	% 0 π cells	Avg (±SD) number of π cells	% WT (10–14π)	% 0 π cells	% 13+ π cells	Avg (±SD) number of π cells	
lin-11::gfp	[a]57	[a]14	4.3 (±2.8)	91	0	0	11.1 (±3.3)	35
lin-11::gfp; nhr-67(pf88)	19	69	[*]1.3 (±2.4)	5	73	0	[*]0.9 (±1.5)	57
egl-13::gfp	[a]89	[a]11	5.4 (±1.8)	97	0	2	12.0 (±1.5)	138
egl-13::gfp; nhr-67(pf88)	25	50	[*]2.0 (±2.6)	28	51	2	[*]2.4 (±3.3)	59
egl-13::gfp; nhr-67(pf2)	32	32	[*]2.6 (±2.5)	52	6	0	[*]5.6 (±3.6)	74
egl-13::gfp; lin-12(n137gf)	5	21	[*]10.7 (±7.6)	5	0	95	[*]25.1 (±4.8)	52
egl-13::gfp; lin-12(n137gf); nhr-67 (pf2)	14	36	[*]3.0 (±4.5)	50	12	31	[*]8.8 (±5.4)	63

Percentages do not necessarily sum to 100% because intermediate results (e.g. 1–4 π cells) are not shown.
[*] Significantly different from transgene alone at $p<0.05$.
[a] Time of onset of *lin-11::gfp* and *egl-13::gfp* expression in the π lineage was variable among animals.

animals, the π descendants were located in irregular positions (e.g., grouped together to one side or the other of the vulva), indicating that even those π descendants that express *egl-13* are defective. The penetrance of the π lineage defect was stronger than the VU to AC conversion defect due to *nhr-67* function in the AC–VU decision, suggesting that loss of one VU cell is not sufficient by itself to explain the defect in the π cells. In some *nhr-67* mutant late L3 and early L4 animals we observed one or more cells with π-like location and appearance by DIC microscopy that did not express *egl-13::gfp* and some early L4 animals that appeared to have undergone the dorsal–ventral division typical of π cells, but did not express *egl-13::gfp* (data not shown). However, in other early L4 mutants that displayed no *egl-13::gfp* expression we were not able to identify obvious candidate post-division π cells. Therefore, we infer that *nhr-67* mutants are defective in the production of the AC signal to π cells and/or at a relatively early step in the π cell response to the AC signal.

A possible explanation for the π lineage defect is that it is a secondary consequence of the earlier defect in AC differentiation. In particular, the loss of LAG-2 expression in the AC could account for the defects in π identity. In order to test this possibility, we examined the effect of *nhr-67* mutations on ventral uterine cells that have been induced to form π cells independent of the AC and LAG-2 signal. A gain-of-function mutation (*n137gf*) in the *lin-12* receptor causes the AC to adopt the VU identity due to inappropriate activation of putative *lin-12* targets in the AC (Greenwald et al., 1983; Wilkinson et al., 1994). Despite the absence of the AC, *lin-12* is activated in the presumptive π and ρ cells, leading to ρ cells being converted into π cells independent of the AC and LAG-2 signal (Newman et al., 1995). As a result, the number of uterine cells that express *egl-13* in early L4 larvae is increased from an average of 12.0 cells in wild-type animals to 25.1 in *lin-12*(*n137*) animals (Table 4; Figs. 7E, F). We examined if an *nhr-67* mutation could suppress the *lin-12*(*gf*) phenotype by constructing an *nhr-67*(*pf2*)*; lin-12*(*n137gf*) strain that carries an *egl-13::gfp* reporter. The strain was strongly suppressed for the *lin-12*(*gf*) effect on π cells (Table 4; Fig. 7G), indicating that the reduction of *nhr-67* is more than sufficient to reverse the effect of the *lin-12*(*gf*) mutation on π cell fate. This result demonstrates that AC-independent *lin-12* activation of the π lineage depends on *nhr-67*. While *nhr-67* function in AC differentiation and *lag-2* expression may contribute to the defect in *nhr-67*-mutant π cells, *nhr-67* must also play an important role in the π cells themselves or in the VU cells that serve as π cell precursors.

The suppression of *lin-12*(*gf*) by *nhr-67*(*pf2*) mutants might be accounted for by *nhr-67* being a downstream regulatory target of *lin-12* signaling in the π cells. If this is the case, however, we would expect a loss of *nhr-67* expression in the presumptive π cells when *lin-12* signaling is compromised. Loss-of-function mutations in *lin-12* cause a phenotype opposite to the gain-of-function mutation: two AC's, extra ρ lineages and no π lineages (Greenwald et al., 1983; Newman et al., 1995). Animals carrying the *nhr-67::gfp* were subjected to *lin-12* (*RNAi*) to examine the consequences of *lin-12* knockdown on *nhr-67* expression. As expected, animals with reduced *lin-12* activity displayed two brightly fluorescing AC's in L2 and L3 animals (Table 3). However, expression of *nhr-67::gfp* in uterine precursor cells adjacent to the AC in L3 was not significantly different from wild-type. We obtained similar results when we explored the effects of the loss of other *Notch* pathway mediators. The *lag-1* gene encodes a transcription factor that mediates *lin-12* signaling (Christensen et al., 1996; Henderson et al., 1994; Tax et al., 1994). Animals bearing the *nhr-67::gfp* and subjected to *lag-1*(*RNAi*) displayed the expected 2 AC phenotype, but did not have altered *nhr-67::gfp* expression in L3 VU-derived cells (Table 3). Likewise, mutations in the *sel-12* γ-secretase, which is required for *lin-12* signaling in the AC-π decision but not the AC–VU decision (Cinar et al., 2001; Levitan and Greenwald, 1995; Li and Greenwald, 1997), did not significantly affect *nhr-67::gfp* expression in L3 VU-derived cells. Taken together, these data suggest that *nhr-67* is not a significant transcriptional regulatory target of the *lin-12* response in π cells.

nhr-67 is required for the expression of lin-12 in the VU and π cells

The expression of *nhr-67::gfp* in the VU cells in mid-L2 animals suggested that *nhr-67* might function in VU development prior to the AC–VU signal. Because the *lin-12/Notch* receptor plays a central role in both AC–VU and AC-π signaling, we examined expression of *lin-12::gfp* in the developing gonad of *nhr-67* mutants. In most mid to late-stage L2 animals, a *lin-12::gfp* transgene was expressed in 2–4 cells of the AC/VU group (average 2.8), but no other gonadal cells (Fig. 8A). In *nhr-67*(*pf88*) and *nhr-67*(*pf159*) mutants, expression in all four AC/VU cells was very rarely observed (average 0.4 cells for both mutants) and was undetectable in 89% of late L2 larva examined (Fig. 8B). We conclude that *nhr-67* is a key regulator of *lin-12* expression in the VU cells. Therefore, the defect in AC–VU signaling apparently reflects the combined effects of the loss of LAG-2 in the AC and loss of LIN-12 in the VU cell.

We also tested the possibility that expression of the *lin-12/Notch* receptor in the L3 π cells and other VU descendants depended on *nhr-67*. A *lin-12::gfp* reporter was expressed in 8–24 VU descendants (average = 13.8) during the L3 stage (Fig. 8C). The *nhr-67*(*pf88*) and *nhr-67*(*pf159*) mutants expressed *lin-12::gfp* in a range of only 0–12 VU descendants (average = 4.3 and 2.9, respectively), with 48% of mutant L3 animals displaying no detectable *lin-12::gfp* expression (Fig. 8D). When expression of *lin-12::gfp* was detected, it was often weak and found only in the more distal VU descendants rather than the π lineage cells. These results demonstrate that expression of *lin-12* in the π cells depends on *nhr-67*, but not vice versa. Therefore, suppression of *lin-12*(*gf*) by *nhr-67* in the π lineage may result entirely or in large part from the failure to express the gain-of-function protein in the absence of *nhr-67*.

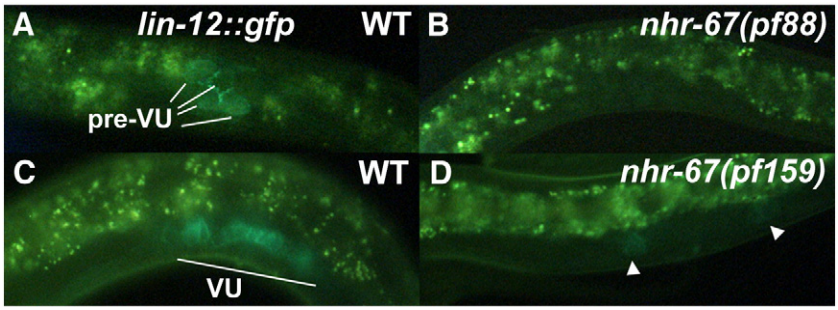

Fig. 8. Expression of *lin-12*/*Notch* depends on *nhr-67*. Fluroescence microscopy showing *lin-12::gfp* expression in wild-type (A, C) and *nhr-67* mutant (B, D) larvae. (A, B) shows early *lin-12* expression in the pre-VU cells of L2 larvae. (C, D) shows later *lin-12* expression in L3 larvae. Arrowheads (D) identify weak *lin-12::gfp* expression in distal extents of the expanding ventral uterine region; note the absence of *lin-12::gfp* in the proximal VU descendants.

Discussion

nhr-67 plays multiple roles in ventral uterine development

Our analysis of *nhr-67* function in *C. elegans* uterine development is consistent with roles at multiple steps and times. First, we propose that *nhr-67* functions in the differentiation of the AC, possibly in conjunction with *hlh-2* and *egl-43*, and is a key regulator of *lin-12* expression in L2 VU cells. The defects in *lag-2* and *zmp-1* expression in the AC that result from *nhr-67* loss-of-function indicate that differentiation of the AC requires *nhr-67*. Loss of *nhr-67* causes defects in AC differentiation that are strikingly similar to those caused by loss of *egl-43* (Fig. 5; Rimann and Hajnal, 2007; Hwang et al., 2007). Taken together, the requirement for *nhr-67* in both AC and VU cell types that are produced from the 4 pre-VU cells suggests that *nhr-67* is an important regulatory factor for differentiation of both cell types.

Second, *nhr-67* is required for the AC–VU decision in L2 larvae. This conclusion is supported by the 2 AC phenotype observed in *nhr-67* mutants and RNAi experiments (Fig. 5; Table 2). As judged by multiple markers of AC identity (*lin-3*, *cdh-3*, *zmp-1* and *egl-43*) the loss of *nhr-67* results in the VU cell adopting an AC identity, which is consistent with a defect in LAG-2 to LIN-12 signaling. It is possible that the defect in AC–VU signaling is entirely due to the loss of *lag-2* expression in the AC and loss of *lin-12* expression in the VU cells. Thus it may not reflect an immediate role for *nhr-67* in the L2 AC–VU signaling event itself, but rather a requirement for *nhr-67* in the differentiation of all four pre-VU cells at an earlier developmental event.

Third, *nhr-67* is required for the development of the π cells of L3 larvae. The loss of expression of key early markers of the π lineage demonstrates that *nhr-67* is required for an early step in π lineage development (Fig. 7; Table 4). Because the induction of the π cells is a relatively late event that depends on both AC identity and VU identity at earlier stages (Newman et al., 1995; 1996; Oommen and Newman, 2007), it is likely that the effect we observe on *nhr-67* mutant π lineage reflects the additive consequence of the requirement for *nhr-67* at several steps. LAG-2 appears to be the ligand for AC-π signaling (Newman et al., 2000), so the defect in π development in *nhr-67* mutants may reflect in part compromised *lag-2* expression in the AC. However, the ability of a relatively weak *nhr-67* mutation (*pf2*) to strongly suppress the *lin-12*(*gf*) π lineage defects indicates that *nhr-67* functions in either VU or π lineages as well, since *lin-12*(*gf*) mutants have no AC's and the *lin-12*(*gf*) effect is not ligand-dependent. The loss of *lin-12* expression in L3 VU descendants may be sufficient to explain this phenotype.

The loss of *lin-12::gfp* expression in *nhr-67* mutants is the most penetrant and earliest consequence we have observed, indicating that *nhr-67* is required for the development of all four pre-VU cells. This raises the possibility that the development of both ρ and π lineage cells might depend on *nhr-67*, since both lineages are derived from the four pre-VU cells. A lack of early markers for ρ cell identities has prevented us from directly addressing the effect of *nhr-67* mutations on ρ cell development, but adult structures derived from ρ lineage cells, such as the spermatheca, and expression of *ser-2::gfp* in mature ρ descendants, do not appear to be significantly affected (data not shown). The consequences of loss of *nhr-67* appear to fall most heavily on the AC–VU decision and π lineage, both of which require *lin-12* signaling. In contrast, the ρ lineage can be executed without an AC and without *lin-12* (Newman et al., 1995). Therefore, it is possible that the function of *nhr-67* is primarily the regulation of components of *lin-12*-related signaling components and AC differentiation.

nhr-67 functions in transcription factor pathways that regulate uterine development

nhr-67 functions in defined pathways that have been previously shown to play key roles in the development of the ventral uterus. We propose that *nhr-67* functions in a pathway with *hlh-2*/*daughterless* and *egl-43*/*Evi1*, and upstream of *lag-2* and *zmp-1* in AC development, and upstream of *lin-12* in VU development. The presence of two evolutionarily conserved CACCTG "E-box" sites in the region removed by the *nhr-67* promoter deletions (Fig. 2) raises the possibility that HLH-2 could be a direct regulator of *nhr-67* transcription in the AC. These particular sites are demonstrated targets for HLH-2/HLH-4 and HLH-2/HLH-10 heterodimers *in vitro* (Grove et al., 2009). In addition, the loss of *hlh-2* causes a more severe phenotype, conversion of the AC into a VU cell (Karp and Greenwald, 2004), as compared to the partial differentiation defect we observe in *nhr-67* mutants. This difference in strength of phenotype also suggests that *hlh-2* may function upstream of *nhr-67*. The regulatory relationship between *egl-43* and *nhr-67* is not clear from our data, since compromising either gene causes a reciprocal change in the expression of the other (Tables 2 and 4). The putative promoter regions of *nhr-67* and *egl-43* do not have conserved binding sites that match the known binding activities of the other protein, so a regulatory relationship between them may not be direct. *zmp-1* has three and *lin-12* has one evolutionarily conserved monomeric AAGTCA NHR-67 binding sites within 2 kb upstream of the predicted start of transcription (B.W., unpublished; DeMeo et al., 2008), raising the possibility that some of the potential regulatory targets of *nhr-67* could be direct. Both *lin-11* and *egl-13* have promoter regulatory regions that have been shown to drive expression in the π lineage (Gupta and Sternberg, 2002; Oommen and Newman, 2007). Both these regions contain well-conserved TAGTCA and TTGTCA sequences (B.W., unpublished), which are related to the defined *nhr-67* binding site, raising the possibility that *nhr-67* could be a direct transcriptional regulator of both genes.

Comparison to nhr-67 function in other tissues

nhr-67 plays multiple, apparently unrelated, roles in *C. elegans* development, just as *tailless* plays multiple roles in *Drosophila* development (Daniel et al., 1999; Pignoni et al., 1990). Sarin et al. (2009) showed that *nhr-67* plays a key role in regulating the left/right

asymmetric identity of the ASE neurons, demonstrating that as for *Drosophila tailless* and vertebrate Tlx, *nhr-67* plays an important function in neuron development. They also found that NHR-67 directly regulates the transcription of the homeobox gene, *cog-1* via a conserved canonical AAGTCA binding site. This is unlikely to be a regulatory interaction that is relevant to our study of ventral uterine development, since *cog-1* is not expressed in the AC or VU lineages (Palmer et al., 2002), although it is possible that *nhr-67* could function to repress expression of *cog-1* in the ventral uterus.

Fernandes and Sternberg (2007) described a role for *nhr-67* in a circuit of transcription factors that regulate gene expression and morphogenesis in the vulva. The vulval cells express some of the same genes as ventral uterine cells, and they found that *nhr-67* was required for the expression of *zmp-1* in the VulA cell and *lin-3* in the VulF cell, but did not find a requirement for *lin-11* expression in any vulva cells. Therefore, their results overlap with ours, identifying vulval regulatory requirements for *nhr-67* in the uterus that are both like those we have described (*zmp-1*) and different from those we have described (*lin-3* and *lin-11*) in the uterus.

Kato and Sternberg (2009) showed that *nhr-67* is expressed in the male linker cell (LC), where it functions in the timing of changes in the direction of migration of the LC during male gonadogenesis. The LC is the male equivalent of the hermaphrodite AC, generated by reciprocal signaling mediated by *lin-12* between the same two gonadal precursors (Greenwald et al., 1983; Kimble and Hirsh, 1979). In males, the LC migrates along a stereotyped pattern to create the overall shape of the male gonad, eventually connecting to the cloaca at the tail. Thus it undergoes a long-range migration unlike the AC. They also found that *nhr-67* is required for expression of *zmp-1* in the male LC, similar to the requirement we have described in the hermaphrodite AC. However, *nhr-67* does not appear to function in the specification of the LC, since a two LC phenotype analogous to the two AC phenotype in the *nhr-67* mutant hermaphrodite was not observed in males. Therefore, while positive regulation of *zmp-1* is a feature of *nhr-67* function in the hermaphrodite AC, hermaphrodite vulva, and male LC, the function of *nhr-67* in gonadogenesis appears to have diverged somewhat between the two sexes.

Implications for conserved tailless function and regulation

The common thread in NR2E1/NR2E2 function across phylogeny is a role in neuron development, suggesting that this is an ancestral function. The *tailless* gene got its name in *Drosophila* on the basis of its key role in patterning the termini of embryos. While we have identified a tail morphology defect in *nhr-67* coding-region deletion homozygotes (Fig. 3B), our observation that all regions of larvae can display cuticle morphology defects in later larva carrying *nhr-67* promoter deletions suggests that *nhr-67* may not have a region-specific function in nematode patterning (Fig. 3C). *tailless* and its orthologs appear to be pleiotropic regulators of animal development with several exaptations to various developmental programs in different species.

Our study suggests a parallel between regulatory pathways in nematode uterine development and regulation of vertebrate neural stem cell identity, which also depends on *Notch*, *daughterless*, and Tlx (Bertrand et al., 2002; Shi et al., 2008). Tlx is a repressor that coordinately prevents differentiation into glial cell types and maintains vertebrate neuronal stem cells in the cell cycle (Shi et al., 2004; Zhang et al., 2006). The *nhr-67* AC–VU phenotype is conceptually analogous to the effect of the loss of Tlx in vertebrate stem cell lines: in both cases the loss of gene function results in a cell that should proliferate (VU in the case of *nhr-67*) exiting the cell cycle and differentiating (becoming AC).

Extensive research in *Drosophila* embryogenesis also connects proneural bHLH regulation and *Notch* signaling to control of neural development (Bertrand et al., 2002; Cummings and Cronmiller, 1994; Jan and Jan, 1993). *nhr-67* and *lin-12* in worms may function in pathways that are analogous to those of the proneural bHLH genes and *Notch* in flies. The regulation of *nhr-67*, high in the *lag-2*-expressing AC and low in the *lin-12*-expressing VU, parallels that of the *Drosophila* proneural bHLH genes. Furthermore, *lag-2* expression depends on *nhr-67*, just as *Delta* expression depends on proneural bHLH genes (Artavanis-Tsakonas et al., 1999; Bertrand et al., 2002). Thus *nhr-67* appears to function analogously to the proneural genes in regulating AC development, raising the possibility that *tll* in flies and Tlx in vertebrates may also play parallel roles in neurogenic pathways.

Supplementary materials related to this article can be found online at doi:10.1016/j.ydbio.2011.06.007.

Acknowledgments

Iva Greenwald and Meera Sundaram provided helpful advice on the manuscript. We thank other members of the *C. elegans* community who provided advice and/or reagents: Robert Barstead, Marc Edgley, Chris Gissendanner, Alex Hajnal, Wendy Hanna-Rose, Oliver Hobert, Shohei Mitani, Johanna Ohlmeyer, Ivo Rimann, Sumeet Sarin, Ann Sluder, Craig Stone, and Paul Sternberg. The *Caenorhabditis* Genetics Center, the *C. elegans* Gene Knockout Consortium, and the National Bioresource Project of Japan provided strains. Other undergraduate students made important contributions to this project: Genna Albert, Alex Breiding, Valerie Brown, Andrea Cerrone, Annie Jilozian, Ryan Kennedy, Bryn Lipovsky, Sonya Martinez-Hunsicker, Jill Neiman, Rick Oravec, Corrine Rennig, Michael Twardzik, and Alberta Yen. Marten Edwards, Amy Hark, and Jeremy Teissere provided advice and generously shared resources. EV, JS and RR received support from NSF REU awards. AW was supported by an award from Merck/AAAS. SJ and BL were funded by the Pasteur Institute. This project was funded by NSF Research at Undergraduate Institution grants IOS-0640483 and IOS-0949367 to BW and EM.

References

Ahringer, J., (ed.), 2006. Reverse genetics, in: WormBook (ed.), The *C. elegans* Research Community, WormBook, doi:10.1895/wormbook.1.47.1.

Artavanis-Tsakonas, S., Rand, M.D., Lake, R.J., 1999. Notch signaling: cell fate control and signal integration in development. Science 284, 770–776.

Bertrand, N., Castro, D.S., Guillemot, F., 2002. Proneural genes and the specification of neural cell types. Nat. Rev. Neurosci. 3, 517–530.

Brenner, S., 1974. The genetics of *Caenorhabditis elegans*. Genetics 77, 71–94.

Cheung, I., Schertzer, M., Rose, A., Lansdorp, P.M., 2002. Disruption of dog-1 in *Caenorhabditis elegans* triggers deletions upstream of guanine-rich DNA. Nat. Genet. 31, 405–409.

Christensen, S., Kodoyianni, V., Bosenberg, M., Friedman, L., Kimble, J., 1996. *lag-1*, a gene required for *lin-12* and *glp-1* signaling in *Caenorhabditis elegans*, is homologous to human CBF1 and *Drosophila* Su(H). Development 122, 1373–1383.

Cinar, H.N., Sweet, K.L., Hosemann, K.E., Earley, K., Newman, A.P., 2001. The SEL-12 presenilin mediates induction of the *Caenorhabditis elegans* uterine π cell fate. Dev. Biol. 237, 173–182.

Cox, G., Kusch, M., Edgar, R.S., 1981. Cuticle of *Caenorhabditis elegans*: its isolation and partial characterization. J. Cell Biol. 90, 7–17.

Cummings, C.A., Cronmiller, C., 1994. The *daughterless* gene functions together with *Notch* and *Delta* in the control of ovarian follicle development in *Drosophila*. Development 120, 381–394.

Daniel, A., Dumstrei, K., Lengyel, J.A., Hartenstein, V., 1999. The control of cell fate in the embryonic visual system by atonal, tailless and EGFR signaling. Development 126, 2945–2954.

DeMeo, S., Lombel, R., Snowflack, D., Smith, E., Reinert, K., Cronin, M., Clever, S., Wightman, B., 2008. Specificity of DNA-binding by the FAX-1 and NHR-67 nuclear receptors of *Caenorhabditis elegans* is partially mediated via a subclass-specific P-box residue. BMC Mol. Biol. 9, 2.

Edgley, M., D'Souza, A., Moulder, G., McKay, S., Shen, B., Gilchrist, E., Moerman, D., Barstead, R., 2002. Improved detection of small deletions in complex pools of DNA. Nucleic Acids Res. 30, e52.

Eisner, T., Eisner, M., Deyrup, M., 1996. Millipede defense: use of detachable bristles to entangle ants. Proc. Natl. Acad. Sci. U.S.A. 93, 10848–10851.

Fernandes, J.S., Sternberg, P.W., 2007. The *tailless* ortholog *nhr-67* regulates patterning of gene expression and morphogenesis in the *C. elegans* vulva. PLoS Genet. 3, e69.

Garriga, G., Guenther, C., Horvitz, H.R., 1993. Migrations of the *Caenorhabditis elegans* HSNs are regulated by *egl-43*, a gene encoding two zinc finger proteins. Genes Dev. 7, 2097–2109.

Gissendanner, C.R., Crossgrove, K., Krauss, K.A., Maina, C.V., Sluder, A.E., 2004. Expression and function of conserved nuclear receptor genes in *Caenorhabditis elegans*. Dev. Biol. 266, 399–416.

Gontijo, A.M., Aubert, S., Roelens, I., Lakowski, B., 2009. Mutations in genes involved in nonsense mediated decay ameliorate the phenotype of *sel-12* mutants with amber stop mutations in *Caenorhabditis elegans*. BMC Genet. 10, 14.

Greenwald, I.S., Sternberg, P.W., Horvitz, H.R., 1983. The *lin-12* locus specifies cell fates in *Caenorhabditis elegans*. Cell 34, 435–444.

Grove, C.A., De Masi, F., Barrasa, M.I., Newburger, D.E., Alkema, M.J., Bulyk, M.L., Walhout, A.J., 2009. A multiparameter network reveals extensive divergence between *C. elegans* bHLH transcription factors. Cell 138, 314–327.

Gupta, B.P., Sternberg, P.W., 2002. Tissue-specific regulation of the LIM homeobox gene *lin-11* during development of the *Caenorhabditis elegans* egg-laying system. Dev. Biol. 247, 102–115.

Hanna-Rose, W., Han, M., 1999. COG-2, a Sox domain protein necessary for establishing a functional vulval-uterine connection in *Caenorhabditis elegans*. Development 126, 169–179.

Henderson, S.T., Gao, D., Lambie, E.J., Kimble, J., 1994. *lag-2* may encode a signaling ligand for the GLP-1 and LIN-12 receptors of *C. elegans*. Development 120, 2913–2924.

Hoyt, P.R., Bartholomew, C., Davis, A.J., Yutzey, K., Gamer, L.W., Potter, S.S., Ihle, J.N., Mucenski, M.L., 1997. The *Evi1* proto-oncogene is required at midgestation for neural, heart, and paraxial mesenchyme development. Mech. Dev. 65, 55–70.

Hwang, B.J., Sternberg, P.W., 2004. A cell-specific enhancer that specifies *lin-3* expression in the *C. elegans* anchor cell for vulval development. Development 131, 143–151.

Hwang, B.J., Meruelo, A.D., Sternberg, P.W., 2007. *C. elegans* EVI1 proto-oncogene, EGL-43, is necessary for Notch-mediated cell fate specification and regulates cell invasion. Development 134, 669–679.

Inoue, T., Sherwood, D.R., Aspöck, G., Butler, J.A., Gupta, B.P., Kirouac, M., Wang, M., Lee, P.Y., Kramer, J.M., Hope, I., Bürglin, T.R., Sternberg, P.W., 2002. Gene expression markers for *Caenorhabditis elegans* vulval cells. Gene Expr. Patterns 2, 235–241.

Jan, Y.N., Jan, L.Y., 1993. HLH proteins, fly neurogenesis, and vertebrate myogenesis. Cell 75, 827–830.

Jansen, G., Hazendonk, E., Thijssen, K.L., Plasterk, R.H., 1997. Reverse genetics by chemical mutagenesis in *Caenorhabditis elegans*. Nat. Genet. 17, 119–121.

Jürgens, G., Kluding, H., Nüsslein-Volhard, C., Wieschaus, E., 1984. Mutations affecting the pattern of the larval cuticle in *Drosophila melanogaster*. II. Zygotic loci on the third chromosome. Wilhem Roux Arch. Dev. Biol. 195, 359–377.

Karp, X., Greenwald, I., 2003. Post-transcriptional regulation of the E/Daughterless ortholog HLH-2, negative feedback, and birth order bias during the AC/VU decision in *C. elegans*. Genes Dev. 17, 3100–3111.

Karp, X., Greenwald, I., 2004. Multiple roles for the E/Daughterless ortholog HLH-2 during *C. elegans* gonadogenesis. Dev. Biol. 272, 460–469.

Kato, M., Sternberg, P.W., 2009. The *C. elegans tailless/Tlx* homolog *nhr-67* regulates a stage-specific program of linker cell migration in male gonadogenesis. Development 136, 3907–3915.

Kimble, J., Hirsh, D., 1979. The postembryonic cell lineages of the hermaphrodite and male gonads in *Caenorhabditis elegans*. Dev. Biol. 70, 396–417.

Kimble, J., Simpson, P., 1997. The LIN-12/Notch signaling pathway and its regulation. Ann. Rev. Cell Dev. Biol. 13, 333–361.

Krause, M., Park, M., Zhang, J.M., Yuan, J., Harfe, B., Xu, S.Q., Greenwald, I., Cole, M., Paterson, B., Fire, A., 1997. A *C. elegans* E/*Daughterless* bHLH protein marks neuronal but not striated muscle development. Development 124, 2179–2189.

Kruisselbrink, E., Guryev, V., Brouwer, K., Pontier, D.B., Cuppen, E., Tijsterman, M., 2008. Mutagenic capacity of endogenous G4 DNA underlies genome instability in FANCJ-defective *C. elegans*. Curr. Biol. 18, 900–905.

Lakowski, B., Eimer, S., Göbel, C., Böttcher, A., Wagler, B., Baumeisterm, R., 2003. Two suppressors of *sel-12* encode C2H2 zinc-finger proteins that regulate presenilin transcription in *Caenorhabditis elegans*. Development 130, 2117–2128.

Levitan, D., Greenwald, I., 1995. Facilitation of lin-12-mediated signalling by sel-12, a *Caenorhabditis elegans* S182 Alzheimer's disease gene. Nature 377, 351–354.

Li, X., Greenwald, I., 1997. HOP-1, a *Caenorhabditis elegans* presenilin, appears to be functionally redundant with SEL-12 presenilin and to facilitate LIN-12 and GLP-1 signaling. Proc. Natl. Acad. Sci. U.S.A. 94, 12204–12209.

Lopingco, M.C., Perkins, A.S., 1996. Molecular analysis of Evi1, a zinc finger oncogene involved in myeloid leukemia. Curr. Top. Microbiol. Immunol. 211, 211–222.

Mackenzie, J., Garcea, R.L., Zengel, J.M., Epstein, H.F., 1978. Muscle development in *Caenorhabditis elegans* mutants exhibiting retarded sarcomere construction. Cell 15, 751–762.

Mello, C., Fire, A., 1995. DNA transformation. Methods Cell Biol. 48, 451–482.

Monaghan, A.P., Bock, D., Gass, P., Schwager, A., Wolfer, D.P., Lipp, H.P., Schutz, G., 1997. Defective limbic system in mice lacking the *tailless* gene. Nature 390, 515–517.

Morrill, J.P., 1986. Scanning electron microscopy of embryos. Methods Cell Biol. 27, 263–293.

Newman, A.P., Sternberg, P.W., 1996. Coordinated morphogenesis of epithelia during development of the *Caenorhabditis elegans* uterine-vulval connection. Proc. Natl. Acad. Sci. U.S.A. 93, 9329–9333.

Newman, A.P., White, J.G., Sternberg, P.W., 1995. The *Caenorhabditis elegans lin-12* gene mediates induction of uterine specialization by the anchor cell. Development 121, 263–271.

Newman, A.P., White, J.G., Sternberg, P.W., 1996. Morphogenesis of the *C. elegans* hermaphrodite uterus. Development 122, 3617–3626.

Newman, A.P., Acton, G.Z., Hartwieg, E., Horvitz, H.R., Sternberg, P.W., 1999. The *lin-11* LIM domain transcription factor is necessary for morphogenesis of *C. elegans* uterine cells. Development 126, 5319–5326.

Newman, A.P., Inoue, T., Wang, M., Sternberg, P.W., 2000. The *Caenorhabditis elegans* heterochronic gene *lin-29* coordinates the vulval-uterine-epidermal connections. Curr. Biol. 10, 1479–1488.

Oommen, K.S., Newman, A.P., 2007. Co-regulation by Notch and Fos is required for cell fate specification of intermediate precursors during *C. elegans* uterine development. Development 134, 3999–4009.

Palmer, R.E., Inoue, T., Sherwood, D.R., Jiang, L.I., Sternberg, P.W., 2002. *Caenorhabditis elegans cog-1* locus encodes GTX/Nkx6.1 homeodomain proteins and regulates multiple aspects of reproductive system development. Dev. Biol. 252, 202–213.

Peixoto, C., Alves, L.C., deMelo, J.V., deSouza, W., 2000. Ultrastructural analyses of the *Caenorhabditis elegans spt-1*(*sc13*) left roller mutant. J. Parasitol. 86, 269–274.

Pettitt, J., Wood, W.B., Plasterk, R.H., 1996. *cdh-3*, a gene encoding a member of the cadherin superfamily, functions in epithelial cell morphogenesis in *Caenorhabditis elegans*. Development 122, 4149–4157.

Pignoni, F., Baldarelli, R.M., Steingrimsson, E., Diaz, R.J., Patapoutian, A., Merriam, J.R., Lengyel, J.A., 1990. The *Drosophila* gene *tailless* is expressed at the embryonic termini and is a member of the steroid receptor superfamily. Cell 62, 151–163.

Rimann, I., Hajnal, A., 2007. Regulation of anchor cell invasion and uterine cell fates by the *egl-43* Evi-1 proto-oncogene in *Caenorhabditis elegans*. Dev. Biol. 308, 187–195.

Sarin, S., Antonio, C., Tursun, B., Hobert, O., 2009. The *C. elegans* Tailless/TLX transcription factor *nhr-67* controls neuronal identity and left/right asymmetric fate diversification. Development 136, 2933–2944.

Shaham, S., (ed.), 2006. Methods in cell biology, in: WormBook, (ed.), The *C. elegans* Research Community, WormBook. doi:10.1895/wormbook.1.49.1.

Sherwood, D.R., Sternberg, P.W., 2003. Anchor cell invasion into the vulval epithelium in *C. elegans*. Dev. Cell 5, 21–31.

Sherwood, D.R., Butler, J.A., Kramer, J.M., Sternberg, P.W., 2005. FOS-1 promotes basement-membrane removal during anchor-cell invasion in *C. elegans*. Cell 121, 951–962.

Shi, Y., Chichung Lie, D., Taupin, P., Nakashima, K., Ray, J., Yu, R.T., Gage, F.H., Evans, R.M., 2004. Expression and function of orphan nuclear receptor TLX in adult neural stem cells. Nature 427, 78–83.

Shi, Y., Sun, G., Zhao, C., Steward, R., 2008. Neural stem cell self-renewal. Crit. Rev. Oncol. Hematol. 65, 43–53.

Stiernagle, T., 2006. Maintenance of *C. elegans*. In: WormBook (Ed.), The *C. elegans* Research Community. WormBook. doi:10.1895/wormbook.1.101.1.

Tax, F.E., Yeargers, J.J., Thomas, J.H., 1994. Sequence of *C. elegans lag-2* reveals a cell-signalling domain shared with *Delta* and *Serrate* of *Drosophila*. Nature 368, 150–154.

Thompson, J.D., Higgins, D.G., Gibson, T.J., 1994. CLUSTAL W: improving the sensitivity of progressive multiple sequence alignment through sequence weighting, position-specific gap penalties and weight matrix choice. Nucleic Acids Res. 22, 4673–4680.

Timmons, L., Court, D.L., Fire, A., 2001. Ingestion of bacterially expressed dsRNAs can produce specific and potent genetic interference in *Caenorhabditis elegans*. Gene 263, 103–112.

Wilkinson, H.A., Fitzgerald, K., Greenwald, I., 1994. Reciprocal changes in expression of the receptor *lin-12* and its ligand *lag-2* prior to commitment in a *C. elegans* fate decision. Cell 79, 1187–1198.

Youds, J.L., Barber, L.J., Ward, J.D., Collis, S.J., O'Neil, N.J., Boulton, S.J., Rose, A.M., 2008. DOG-1 is the *Caenorhabditis elegans* BRIP1/FANCJ homologue and functions in interstrand cross-link repair. Mol. Cell. Biol. 28, 1470–1479.

Yu, R.T., McKeown, M., Evans, R.M., Umesono, K., 1994. Relationship between *Drosophila* gap gene *tailless* and a vertebrate nuclear receptor Tlx. Nature 370, 375–379.

Zahn, T.R., Macmorris, M.A., Dong, W., Day, R., Hutton, J.C., 2001. IDA-1, a *Caenorhabditis elegans* homolog of the diabetic autoantigens IA-2 and phogrin, is expressed in peptidergic neurons in the worm. J. Comp. Neurol. 429, 127–143.

Zhang, C.L., Zou, Y., Yu, R.T., Gage, F.H., Evans, R.M., 2006. Nuclear receptor TLX prevents retinal dystrophy and recruits the corepressor atrophin1. Genes Dev. 20, 1308–1320.

Zhao, Y., Tarailo-Graovac, M., O'Neil, N.J., Rose, A.M., 2008. Spectrum of mutational events in the absence of DOG-1/FANCJ in *Caenorhabditis elegans*. DNA Repair 7, 1846–1854.